J. Fluid Mech. (2013), *vol.* 717, *pp.* 232–254.
doi:10.1017/jfm.2012.568

Three-vortex quasi-geostrophic dynamics in a two-layer fluid. Part 1. Analysis of relative and absolute motions

M. A. Sokolovskiy[1,2], K. V. Koshel[3,4,†] and J. Verron[5]

[1]Water Problems Institute, RAS, 3, Gubkina Str., Moscow, 119991, Russia

[2]Southern Federal University, 8a Mil'chakova Str., Rostov-on-Don, 344090, Russia

[3]V. I. Il'ichev Pacific Oceanological Institute, FEB RAS, 43 Baltiyskaya Str., Vladivostok, 690041, Russia

[4]Far Eastern Federal University, 8 Sukhanova Str., Vladivostok, 690950, Russia

[5]Laboratoire des Ecoulements Géophysiques et Industriels, CNRS, BP 52, 38041, Grenoble, CEDEX 9, France

(Received 18 March 2012; revised 11 November 2012; accepted 15 November 2012; first published online 1 February 2013)

The results presented here examine the quasi-geostrophic dynamics of a point vortex structure with one upper-layer vortex and two identical bottom-layer vortices in a two-layer fluid. The problem of three vortices in a barotropic fluid is known to be integrable. This fundamental result is also valid in a stratified fluid, in particular a two-layer one. In this case, unlike the barotropic situation, vortices belonging to the same layer or to different layers interact according to different formulae. Previously, this occurrence has been poorly investigated. In the present work, the existence conditions for stable stationary (translational and rotational) collinear two-layer configurations of three vortices are obtained. Small disturbances of stationary configurations lead to periodic oscillations of the vortices about their undisturbed shapes. These oscillations occur along elliptical orbits up to the second order of the Hamiltonian expansion. Analytical expressions for the parameters of the corresponding ellipses and for oscillation frequencies are obtained. In the case of finite disturbances, vortex motion becomes more complicated. In this case we have made a classification of all possible movements, by analysing phase portraits in trilinear coordinates and by computing numerically the characteristic trajectories of the absolute and relative vortex motions.

Key words: baroclinic flows, quasi-geostrophic flows, vortex dynamics

1. Introduction

The problem of three vortices in a two-dimensional layer of an ideal homogeneous incompressible fluid with zero velocity at infinity, originating from the pioneering dissertation work of Gröbli (1877), is the focus of numerous publications, e.g. Poincaré (1893), Synge (1949), Novikov (1976), Aref (1979, 1983, 1989), Meleshko

† Email address for correspondence: kvkoshel@poi.dvo.ru

& Konstantinov (1993), Meleshko & van Heijst (1994), Newton (2001), Boyland, Stremler & Aref (2003) and Gudimenko (2008), and has been exhaustively studied, e.g. Tavantzis & Ting (1988), Borisov & Mamaev (2005), Aref (2009, 2010) and Gudimenko & Zakharenko (2010).

The problem of three vortices is integrable (Meleshko & Konstantinov 1993; Kozlov 1998; Newton 2001; Borisov & Mamaev 2005). However, the four-vortex dynamics is only integrable in the case of initially symmetric vortex locations. Because of impulse conservation, this symmetry property is valid at any time (Aref & Pomphrey 1982; Eckhardt 1988; Eckhardt & Aref 1988; Aref & Stremler 1999; Sokolovskiy & Verron 2000*b*). Chaotic regimes in the problem of four vortices were found for the first time almost simultaneously and independently in the works of Novikov & Sedov (1979*a*,*b*) and Aref & Pomphrey (1980). A rigorous proof of the non-integrability of this problem in the particular case where one of the point vortices has zero intensity, i.e. is a simple fluid particle, was given by Ziglin (1980). Examples of stable and unstable motion of fluid particles (advection) in the vicinity of stable equilibrium configurations of three vortices are shown in an accompanying paper (Koshel, Sokolovskiy & Verron 2013, hereinafter referred to as KSV).

In a two-layer rotating fluid, unlike the barotropic case, vortices belonging to the same layer and vortices located in different layers interact in different ways. The simplest way to show this is the example of a pair of point vortices. In a homogeneous fluid the law $v \sim 1/R$, where R is half the distance between the vortices, is valid for the velocity of a pair, whereas for the two-layer pair, $v \sim [1/R \pm \mathrm{K}_1(R)]$, where K_1 is a modified Bessel function. The positive sign corresponds to the case when both vortices are located in the same layer, and the negative sign to the case when they are located in different layers, i.e. a *heton* (Hogg & Stommel 1985; Sokolovskiy & Verron 2000*a*; Gryanik, Sokolovskiy & Verron 2006; Jamaloodeen & Newton 2007). In the second case, the velocity of a two-layer pair has a non-monotonic character, tending to zero as $R \to 0$ and $R \to \infty$ and taking a maximum value at $R \approx 1.14R_d$, where R_d is the Rossby deformation radius.

It is obvious that baroclinicity plays a very important role in the problem of three vortices. For example, in barotropic fluid, the collinear symmetrical tripolar structure (peripheral vortices are of equal intensity $\kappa > 0$ and a central vortex has the intensity $\mu\kappa$) always rotates around the central vortex in the cyclonic sense when $\mu > -0.5$, and in the anticyclonic sense when $\mu < -0.5$; if $\mu = -0.5$, we have a static condition at any distance R of the peripheral vortices from the central one.

Again, as for the vortex pair, the baroclinic tripole is fundamentally different from the barotropic one. A symmetrical two-layer tripolar structure composed of a central vortex in the upper layer and two identical peripheral vortices in the bottom layer for $\mu < -0.5$ has a static state half the distance value $R = R_\mu$, where R_μ is a function of parameter μ. This vortex structure always rotates in the anticyclonic direction if $R > R_\mu$ (the interlayer interaction is predominant), and it rotates in the cyclonic direction if $R < R_\mu$ (the intralayer interaction between the vortices of the bottom layer predominates).

In a two-layer fluid, the dynamics of three vortices having an arbitrary initial vortex position has not been studied even in the particular case discussed above, when one vortex is in the upper layer and two equal vortices are located in the bottom layer. This work fills this gap. Here, we give a classification of possible motions of such vortex systems, and, in particular, we study in detail its stationary states.

The structure of the paper is as follows. In § 2, we state the problem of the dynamics of point vortices in a two-layer rotating fluid on the f-plane within the

approximation of a rigid lid at the surface, write integral invariants and describe the construction of phase portraits in trilinear coordinates. Most of § 3 is taken up with citing of results on stationary solutions of a three-vortex problem in rotating two-layer fluid taken from Gryanik *et al.* (2006) and Sokolovskiy & Verron (2006), that are necessary for understanding the subsequent material of this article. The new result here is a generalized diagram of the vortex structure state in the plane of geometric parameters (figure 5). In § 4, we construct an approximate solution for the relative trajectories of the vortices, when they deviate slightly from their steady states, using the method of small perturbations. It is shown that the trajectories up to the second order have an elliptical shape. In § 5, we study arbitrary motion of the vortices, give a classification of absolute and relative trajectories, and investigate a frequency dependence of the relative motion of the vortices. Section 6 summarizes the main results.

2. Problem formulation

The equations of motion of a point vortex system in a two-layer inviscid fluid rotating with an angular velocity $f/2$ (f is the constant Coriolis parameter) under the quasi-geostrophic approximation and assuming the rigid lid condition at the surface and a flat bottom have the following non-dimensional form:

$$\dot{x}_j^\alpha = -\frac{h_j}{2\pi}\left\{\sum_{\substack{\beta=1\\ \beta\neq\alpha}}^{A_j}\kappa_j^\beta\frac{y_j^\alpha-y_j^\beta}{\left(r_{jj}^{\alpha\beta}\right)^2}\left[1+\frac{h_{3-j}}{h_j}\gamma r_{jj}^{\alpha\beta}\mathrm{K}_1(\gamma r_{jj}^{\alpha\beta})\right]\right.$$
$$\left.+\sum_{\beta=1}^{A_{3-j}}\kappa_{3-j}^\beta\frac{h_{3-j}}{h_j}\frac{y_j^\alpha-y_{3-j}^\beta}{\left(r_{j(3-j)}^{\alpha\beta}\right)^2}[1-\gamma r_{j(3-j)}^{\alpha\beta}\mathrm{K}_1(\gamma r_{j(3-j)}^{\alpha\beta})]\right\}, \tag{2.1}$$

$$\dot{y}_j^\alpha = \frac{h_j}{2\pi}\left\{\sum_{\substack{\beta=1\\ \beta\neq\alpha}}^{A_j}\kappa_j^\beta\frac{x_j^\alpha-x_j^\beta}{\left(r_{jj}^{\alpha\beta}\right)^2}\left[1+\frac{h_{3-j}}{h_j}\gamma r_{jj}^{\alpha\beta}\mathrm{K}_1(\gamma r_{jj}^{\alpha\beta})\right]\right.$$
$$\left.+\sum_{\beta=1}^{A_{3-j}}\kappa_{3-j}^\beta\frac{h_{3-j}}{h_j}\frac{x_j^\alpha-x_{3-j}^\beta}{\left(r_{j(3-j)}^{\alpha\beta}\right)^2}[1-\gamma r_{j(3-j)}^{\alpha\beta}\mathrm{K}_1(\gamma r_{j(3-j)}^{\alpha\beta})]\right\}. \tag{2.2}$$

Here $r_{ij}^{\alpha\beta}=\sqrt{\left(x_i^\alpha-x_j^\beta\right)^2+\left(y_i^\alpha-y_j^\beta\right)^2}$ is the distance between vortex α with dimensionless circulation κ_i^α within the ith layer and vortex β with dimensionless circulation κ_j^β within the jth layer ($\alpha,\beta=1,2,\ldots,A_j$; $i,j=1,2$); h_1 and h_2 are the thicknesses of the top and bottom layers, respectively (the layers are numbered from top to bottom); $\gamma=D/R_d$ where $R_d=\sqrt{g'h_1h_2/(h_1+h_2)}/f$ is the internal Rossby radius, D is the horizontal scale used to non-dimensionalize x and y, $g'=g(\rho_2-\rho_1)/\rho_0$, where ρ_1, ρ_2 are the densities of the top and bottom layers, ρ_0 is the mean density, and g is the acceleration due to gravity; a dot above a variable means a derivative with respect to time.

The system (2.1)–(2.2), obtained for the first time by Gryanik (1983), inherently represents identities

$$\dot{x}_j=u_j=-\psi_{jy},\quad \dot{y}_j=v_j=\psi_{jx}, \tag{2.3}$$

where ψ_j is a stream function in the jth layer. The easiest way of obtaining the expressions on the right-hand sides of (2.1)–(2.2) is by examining them as a discrete limit of the motion of vortex patches of finite size, excluding the self-influence of the vortex and using known links between Π_j (potential vorticity in layers) and the stream functions:

$$\Pi_j = \nabla^2\psi_j + Fr_j\left(\psi_{3-j} - \psi_j\right), \quad Fr_j = h_{3-j}(h_1 + h_2)/R_d, \quad j = 1, 2. \tag{2.4}$$

Hear, Fr_1, Fr_2 are the Froud numbers.

If the potential vortices in the layers can be represented as

$$\Pi_j = \sum_{\alpha=1}^{A_j} \Pi_j^\alpha(x, y, t), \quad j = 1, 2, \tag{2.5}$$

where Π_j^α are piecewise constant functions nonlinear on the domains S_j^α then the path to the limit is as follows (Gryanik *et al.* 2006):

$$\lim_{\substack{S_j^\alpha \to 0 \\ \Pi_j^\alpha \to \infty}} \Pi_j^\alpha S_j^\alpha = \kappa_j^\alpha. \tag{2.6}$$

The system (2.1)–(2.2) has integral invariants

$$Q = \sum_{j=1}^{2} h_j \sum_{\alpha=1}^{A_j} \kappa_j^\alpha, \quad P_x = \sum_{j=1}^{2} h_j \sum_{\alpha=1}^{A_j} x_j^\alpha \kappa_j^\alpha, \quad P_y = \sum_{j=1}^{2} h_j \sum_{\alpha=1}^{A_j} y_j^\alpha \kappa_j^\alpha, \tag{2.7}$$

$$M = \sum_{j=1}^{2} h_j \sum_{\alpha=1}^{A_j} \left[(x_j^\alpha)^2 + (y_j^\alpha)^2\right] \kappa_j^\alpha, \tag{2.8}$$

representing the total intensity Q, the impulse components P_x and P_y, and the angular momentum M.

The system (2.1)–(2.2) can be written in the Hamiltonian form

$$\dot{q}_j^\alpha = \frac{\partial \mathscr{H}}{\partial p_j^\alpha}, \quad \dot{p}_j^\alpha = -\frac{\partial \mathscr{H}}{\partial q_j^\alpha}, \quad \alpha = 1, 2, \ldots, A^j; j = 1, 2, \tag{2.9}$$

where the canonical variables $q_j^\alpha = x_j^\alpha$ and $p_j^\alpha = y_j^\alpha \kappa_j^\alpha h_j$ are the generalized coordinates and the generalized impulses, respectively.

The Hamiltonian, coinciding with the energy of interaction between vortices, has the form

$$\mathscr{H} = -\frac{1}{4\pi} \sum_{j=1}^{2} h_j \left\{ \sum_{\substack{\alpha,\beta=1 \\ \alpha\neq\beta}}^{A_j} \kappa_j^\alpha \kappa_j^\beta \left[\ln \gamma_* r_{jj}^{\alpha\beta} - \frac{h_{3-j}}{h_j} \mathrm{K}_0(\gamma r_{jj}^{\alpha\beta})\right] \right.$$
$$\left. + \sum_{\alpha,\beta=1}^{A_j, A_{3-j}} \frac{h_{3-j}}{h_j} \kappa_j^\alpha \kappa_{3-j}^\beta [\ln \gamma_* r_{j(3-j)}^{\alpha\beta} + \mathrm{K}_0(\gamma r_{j(3-j)}^{\alpha\beta})] \right\}, \tag{2.10}$$

where $\gamma_* = D/R_{reg}$ and R_{reg} is a regularizing scale of length equal, for example, to the Oboukhov–Rossby scale (Gryanik 1983) or to the radius of the sphere in problems of vortex dynamics on a sphere (Bogomolov 1977, 1985).

It can be easily shown that invariants M, $\mathscr{H}$ and the combination $(P_x)^2 + (P_y)^2$ are pairwise involutive (i.e. the corresponding Poisson brackets are zero), and, according to the Liouville theorem (Kozlov 1996, 1998), in the case of three vortices in a two-layer fluid (this is also true for an N-layer fluid with arbitrary N), as well as in a homogeneous medium (Gröbli 1877; Synge 1949; Aref 1979, 1983, 1989, 2009, 2010; Kimura 1988; Tavantzis & Ting 1988; Aref *et al.* 1989; Rott 1989, 1990; Kozlov 1998; Stremler & Aref 1999; Boyland *et al.* 2003; Borisov & Mamaev 2005; Blackmore, Ting & Knio 2007; Gudimenko 2008; Gudimenko & Zakharenko 2010), the problem always has a regular solution.

Next we assume $A_1 = 1$, $A_2 = 2$ (i.e. we consider a special case of the three-vortex problem with one vortex in the top layer and two vortices in the bottom layer), $h_1 = h_2 = 1/2$, $\kappa_2^1 = \kappa_2^2 = 1$, $\kappa_1^1 = \mu < 0$ and $D = R_d$ or $\gamma = 1$.

For this case, the equations of motion (2.1)–(2.2) in relative variables have the form:

$$\dot{r}_{22}^{12} = \frac{\mu S}{\pi} \frac{(r_{12}^{11})^2[1 - r_{12}^{12}\mathrm{K}_1(r_{12}^{12})] - (r_{12}^{12})^2[1 - r_{12}^{11}\mathrm{K}_1(r_{12}^{11})]}{(r_{12}^{11})^2\,(r_{12}^{12})^2}, \tag{2.11}$$

$$\dot{r}_{12}^{12} = \frac{S}{\pi} \frac{(r_{12}^{11})^2[1 + r_{22}^{12}\mathrm{K}_1(r_{22}^{12})] - (r_{22}^{12})^2[1 - r_{12}^{11}\mathrm{K}_1(r_{12}^{11})]}{(r_{12}^{11})^2\,(r_{22}^{12})^2}, \tag{2.12}$$

$$\dot{r}_{12}^{11} = \frac{S}{\pi} \frac{(r_{22}^{12})^2[1 - r_{12}^{12}\mathrm{K}_1(r_{12}^{12})] - (r_{12}^{12})^2[1 + r_{22}^{12}\mathrm{K}_1(r_{22}^{12})]}{(r_{12}^{12})^2\,(r_{22}^{12})^2}, \tag{2.13}$$

where the value

$$S = \tfrac{1}{2}[y_1^1(x_2^2 - x_2^1) + y_2^1(x_1^1 - x_2^2) + y_2^2(x_2^1 - x_1^1)] \tag{2.14}$$

is equal to the area of the oriented triangle constructed on the coordinates of vortices (x_1^1, y_1^1), (x_2^1, y_2^1), and (x_2^2, y_2^2), with positive sign when the path from the first to the third vortex is in the cyclonic direction, and negative sign when this direction is anticyclonic. From (2.11)–(2.13) it can be seen, in particular, that all collinear configurations ($S = 0$) are stationary. However, as shown below, stable collinear states are only represented by vortex structures satisfying special conditions.

From (2.11)–(2.13) we can readily obtain the identity $\dot{L} = 0$, where

$$L = (r_{22}^{12})^2 + \mu\left[(r_{12}^{12})^2 + (r_{12}^{11})^2\right] \tag{2.15}$$

is a two-layer analogue of the well-known vortex integral (Lamb 1932), which, as well as the Hamiltonian, depends only on the distance between vortices. The first integrals (2.8) become:

$$Q = \tfrac{1}{2}(2 + \mu), \quad P_x = \tfrac{1}{2}\left(x_2^1 + \mu x_1^1 + x_2^2\right), \quad P_y = \tfrac{1}{2}\left(y_2^1 + \mu y_1^1 + y_2^2\right), \tag{2.16a}$$

$$M = \tfrac{1}{2}\left\{\left(x_2^1\right)^2 + \left(y_2^1\right)^2 + \mu\left[\left(x_1^1\right)^2 + \left(y_1^1\right)^2\right] + \left(x_2^2\right)^2 + \left(y_2^2\right)^2\right\}. \tag{2.16b}$$

From (2.15) and (2.16) we can get

$$L = 4\left[QM - (P_x)^2 - (P_y)^2\right]. \tag{2.17}$$

The equality (2.15) allows us to introduce the so-called trilinear coordinates (t_1, t_2, t_3) (Aref 1979), satisfying at $L \neq 0$ the evident equality

$$t_1 + t_2 + t_3 = 3, \tag{2.18}$$

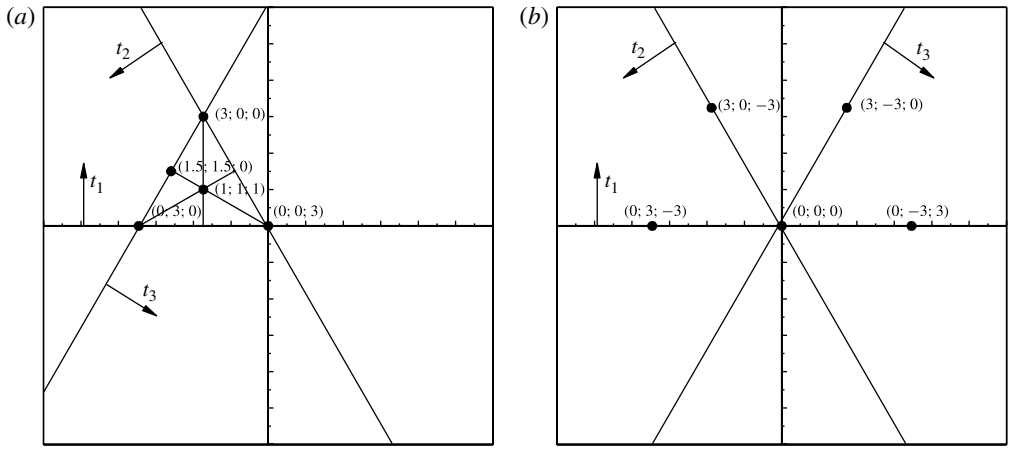

FIGURE 1. Scheme of the trilinear coordinates with specified orientation of axes: (*a*) $L \neq 0$ and (*b*) $L = 0$.

and defined as

$$t_1 = \frac{3\,(r_{22}^{12})^2}{L}, \quad t_2 = \frac{3\mu\,(r_{12}^{12})^2}{L}, \quad t_3 = \frac{3\mu\,(r_{12}^{11})^2}{L}. \tag{2.19}$$

These coordinates characterize the distance from lines constructed on the sides of an equilateral triangle with the height of 3, to any point of the plane (see figure 1*a*).

When $L = 0$ (this occurs only in interval $-2 < \mu < 0$), we have

$$t_1 + t_2 + t_3 = 0 \tag{2.20}$$

and

$$t_1 = 3\,(r_{22}^{12})^2, \quad t_2 = 3\mu\,(r_{12}^{12})^2, \quad t_3 = 3\mu\,(r_{12}^{11})^2. \tag{2.21}$$

A geometric interpretation of the trilinear coordinates for this case is given in figure 1(*b*).

To quantitatively study the dynamic system on the plane of variables (t_1, t_2, t_3) it is reasonable to identify the 'physical domain' (PD), in which the distances between three arbitrary points (point vortices) satisfy the triangle inequality. In terms of trilinear coordinates, this inequality becomes

$$(\mu t_1)^2 + (t_2)^2 + (t_3)^2 \leqslant 2(\mu t_1 t_2 + \mu t_1 t_3 + t_2 t_3). \tag{2.22}$$

Clearly, the points on the boundary of PD (where (2.22) becomes an equality) always correspond to a continuum of collinear states of the three vortices. From (2.22) it follows that when $\mu \geqslant 1$ or $\mu < -2$ the PD is finite, while when $\mu \in [-2; 1)$, the PD is infinite.

Figure 2 gives an example of a phase portrait, i.e. isolines of the Hamiltonian (2.10) in the trilinear coordinates (t_1, t_2, t_3), for the case $\mu = -2.5$. The 'non-physical' domains are shaded. The thick lines are separatrices splitting domains of different types of *relative motion* {1}, {2} and {3}. The main properties of these types of motion are given below (in § 5) along with the appropriate trajectories of vortex motion. Here, we will only mention that, since all isolines of the phase portraits in figure 2 reach the boundary of the PD twice, each of the three types of motion involves two

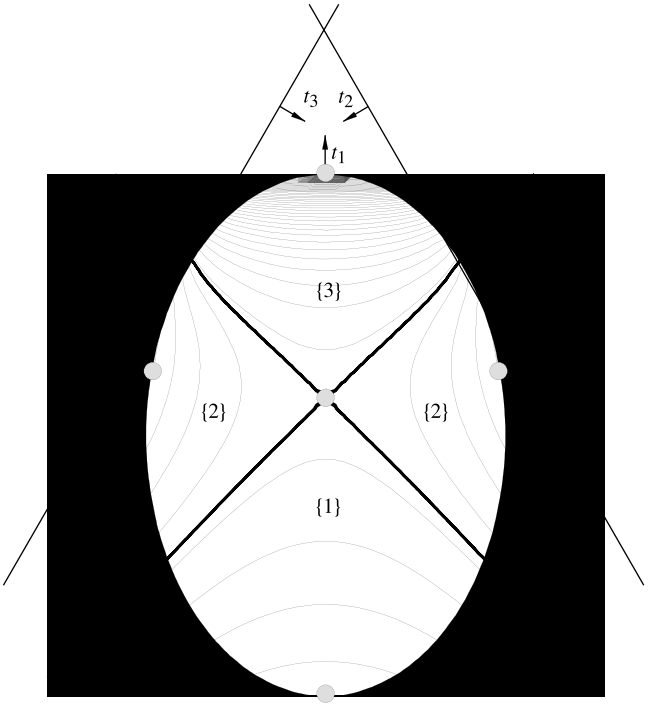

FIGURE 2. Phase portrait in trilinear coordinates (t_1, t_2, t_3) at $\mu = -2.5$. The grey circular symbols indicate elliptic and hyperbolic singular points.

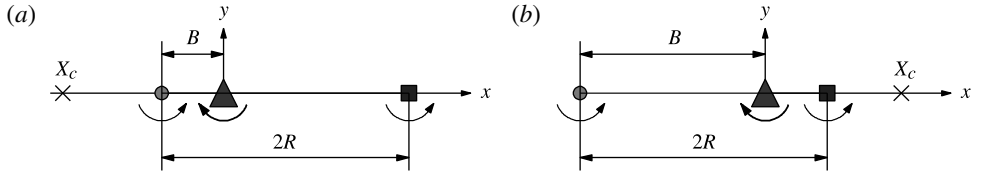

FIGURE 3. Scheme of the initial layout of vortices at $\mu = -2.5$: (*a*) $B < R$ and (*b*) $B > R$. Here and in the figures below, the triangle marks the position of the top-layer vortex and the circle and the square mark the positions of the bottom-layer vortices; X_c is the position of the vorticity centre (3.4). The size of each symbol is proportional to the absolute value of the intensity of the vortex. The arc arrows show the cyclonic or anticyclonic directions of the vortices.

collinear states. During the evolution of the vortex system, the appropriate point of the phase plane oscillates between the boundary points, periodically 'reflecting' from a PD boundary. Thus, all possible motions of such a vortex system can be exhaustively studied, if a collinear state is specified as the initial configuration. In what follows, we suppose that at the initial moment all three vortices lie on a straight line (without loss of generality, we can assume it to be the x-axis), so that the top-layer vortex is situated at the origin of coordinates, as shown in figure 3.

3. Stationary three-vortex structures

As can be seen from figure 2, circular grey symbols indicate the following singular points in the phase portrait.

(i) A hyperbolic point of separatrix intersection.

A non-stable configuration of isosceles triangle shape, containing the upper-layer vortex at the point where lateral sides intersect and the bottom-layer vortices at the angles at the triangle base, corresponds throughout to this point. Because of the instability, the vortex structure takes this position only twice during each period.

(ii) Elliptic points.

(*a*) The upper point of the PD boundary ($R = 0, B \neq 0$) in area {3}.

A limit stationary configuration corresponds to this point, when two equal bottom-layer vortices collapse and rotate around the merging point with theoretically infinite angular velocity, and the whole construction rotates around the centre of vorticity with angular velocity $\omega = (\mu + 2)/4\pi B^2$.

(*b*) The bottom point of the PD boundary ($B = R$) in area {1}.

The axisymmetric collinear tripolar structure, described in the Introduction and named a *roundabout* by Gryanik *et al.* (2006), corresponds to this point. Equations (2.1)–(2.2), written in polar coordinates, allow one to easily obtain an expression for the angular velocity of rotation of the peripheral vortices belonging to the bottom layer around the central vortex of the upper layer:

$$\omega = \frac{1}{4\pi R^2}\left[\frac{1}{2} + \mu(1 - R\mathrm{K}_1(R)) + R\mathrm{K}_1(2R)\right]. \tag{3.1}$$

For $\mu < 0.5$ equation (3.1) for $\omega = 0$ always has a solution $R = R_\mu$ (see the Introduction) giving the static state; for $R > R_\mu$, peripheral vortices rotate in anticyclonic direction initiated by the central vortex (*ordinary roundabout*), and for $R < R_\mu$ they rotate in the opposite direction (*inverse roundabout*).

(*c*) Lateral points of the PD boundary in areas {2}.

Non-trivial non-symmetric collinear three-vortex configurations correspond to these points of the phase portrait. The distances between them satisfy the following equation obtained from (2.12)–(2.13):

$$\frac{1}{2R} + \frac{2R(1+\mu)}{B(2R-B)} + \mathrm{K}_1(2R) + \frac{(2R + B\mu)\mathrm{K}_1(2R - B) - [2R(1+\mu) - B\mu]\mathrm{K}_1(B)}{2(R-B)} = 0. \tag{3.2}$$

This collinear construction rotates as a solid body with the angular velocity

$$\omega = \frac{\mu + 2}{4\pi(2R + B\mu)}\left[\frac{B + 2R\mu}{2BR} - \mu\mathrm{K}_1(B) + \mathrm{K}_1(2R)\right] \tag{3.3}$$

about a vorticity centre with coordinates

$$(X_c, Y_c) = \left(\frac{2(R-B)}{\mu + 2}, 0\right). \tag{3.4}$$

In Sokolovskiy & Verron (2006), such a configuration was called an *eccentric roundabout*. The coordinates of the rotation centre (3.4) satisfy the

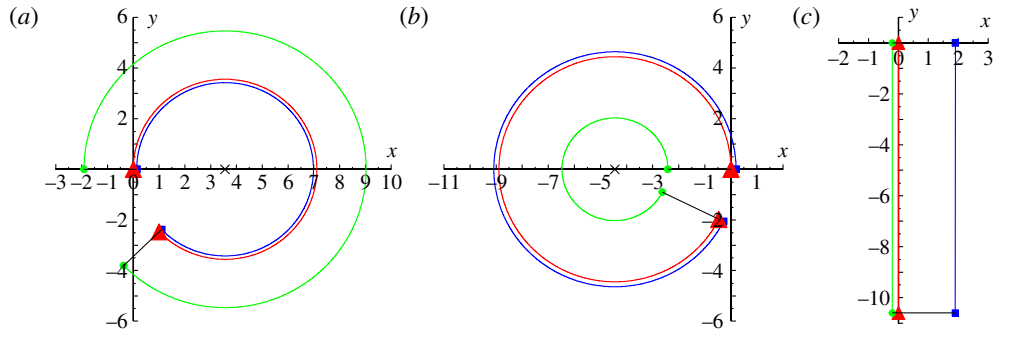

FIGURE 4. Examples of absolute motion trajectories of stationary configurations: (*a*) $\mu = -2.5$ (eccentric roundabout, $X_c > 0$); (*b*) $\mu = -1.5$ (eccentric roundabout, $X_c < 0$); (*c*) $\mu = -2$ (triton, $X_c = \infty$). The initial moment corresponds to a collinear configuration of the three vortices on the x-axis. Crosses on the x-axis are the coordinates for vorticity centres $(X_c, 0)$. Symbols have the same meaning as in figure 3, the red line corresponds to the trajectory of the top-layer vortex, while the green and blue lines correspond to the two bottom-layer vortices.

inequalities

$$X_c \geqslant 0 \quad \text{for } -2 > \mu > -\infty, \quad B \geqslant R \quad \text{or for } -1 \geqslant \mu > -2, \quad R \geqslant B, \tag{3.5a}$$

$$X_c \leqslant 0 \quad \text{for } -1 \geqslant \mu > -2, \quad B \geqslant R \quad \text{or for } -2 > \mu > -\infty, \quad R \geqslant B; \tag{3.5b}$$

when $\mu > -1$, (3.2) has no solutions.

At $\mu = -2$ and $B \neq R$, the angular velocity (3.3) is identically zero, the vorticity centre X_c goes to infinity, the condition (3.2) becomes

$$\frac{B^2 - 2BR + 4R^2}{2BR(2R - B)} - \mathrm{K}_1(B) - \mathrm{K}_1(2R - B) - \mathrm{K}_1(2R) = 0, \tag{3.6}$$

and the motion of the collinear vortex structure becomes translational motion with constant velocity

$$V = \frac{1}{4\pi}\left[\frac{2(R - B)}{B(2R - B)} - \mathrm{K}_1(B) + \mathrm{K}_1(2R - B)\right] \tag{3.7}$$

directed perpendicular to the x-axis. According to the terminology used in Sokolovskiy & Verron (2002*a*,*b*, 2004, 2006), we will refer to such a structure as a *triton*.

Figure 4(*a*,*b*) gives examples of trajectories of absolute motion of the vortices comprising an eccentric roundabout when both B and R satisfy (3.2) (clearly, the signs of X_c satisfy the rules (2.16)), and figure 4(*c*), where the trajectory of the top-layer vortex lies on the y-axis, shows the behaviour of a triton under conditions (3.6). The segments in all cases connect the positions of vortices in the initial and final (calculated) moments. The time intervals for calculation in figure 4(*a*,*b*) are chosen such that the trajectories do not overlap.

Section 4 of this article is dedicated to the study of weakly disturbed stationary solutions of eccentric roundabout type.

Figure 5 gives the solution of (3.2) with $\mu = -2.5$ in the form of the curve $B(R)$, and the dependence of the angular velocity (3.3) and the position of the vorticity

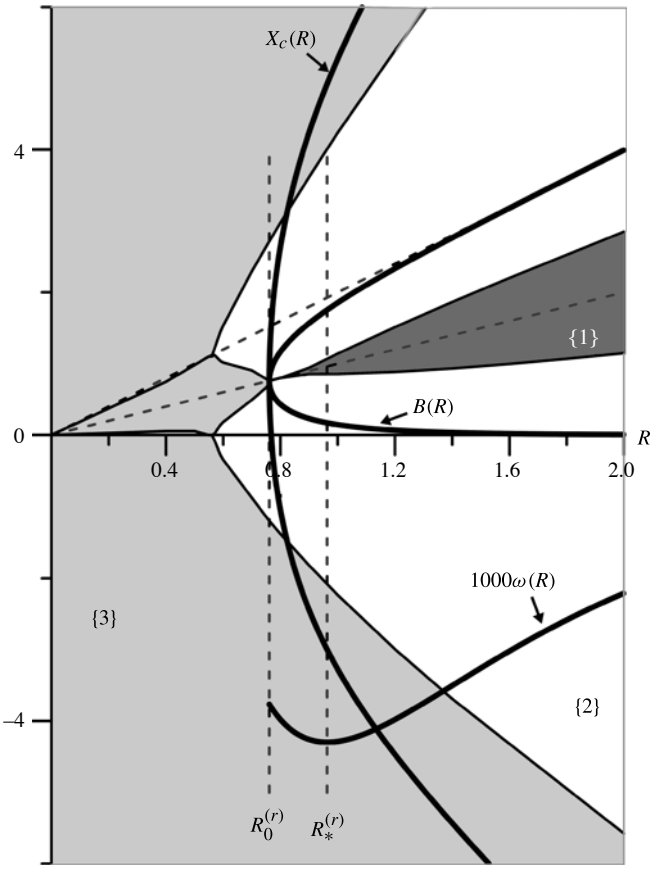

FIGURE 5. Plots of functions $B(R)$, $1000\omega(R)$ and $X_c(R)$ for an eccentric roundabout with $\mu = -2.5$. The sloping dashed lines $B = R$ and $B = 2R$ specify the axis of symmetry of curve (3.2) and asymptotics of their solutions for $R \gg 1$, respectively. The notations {1}, {2} and {3} for the domains, marked by dark grey, white, and light grey, respectively, have the same meaning as in figure 2.

centre (3.4) on R. When $B = R = R_0^{(r)} = 0.7609$ (hereafter, unless the context requires greater detail, we give only four decimal digits, though the calculations were carried out with double precision and yield reliable values up to 10^{-12}), the vorticity centre coincides with the top-layer vortex, and we have an *ordinary roundabout*, rotating with angular velocity $\omega_0 = -0.0038$. At $R = R_*^{(r)} = 0.9630$ and the corresponding values $B_*^{(1)} = 0.1710$ and $B_*^{(2)} = 1.7550$, the angular velocity takes its minimal value $\omega_* = -0.0043$. Notwithstanding the fact that the solution of (3.2) has two branches and the coordinates of the vorticity centre (3.4) change their signs with the replacement of B by R, the angular velocity at $\mu = -2.5$ does not change its sign on the curve $B(R)$.

Note that the domain of existence of solutions of types {1}, {2} and {3} are given here in the coordinates (R, B). The part of the domain {3}, bounded by thick lines within the angle between the straight lines $B = 0$ and $B = 2R$, has the following property: for all R and B belonging to it, the trajectory of the relative motion of the top-layer vortex always lies within domains bounded by closed trajectories of the bottom-layer vortex.

4. Analysis of perturbed motion at small deviations from stationary states

The elliptic type of fixed points corresponding to the solutions considered on phase portraits (figure 2), suggests that they are stable under small perturbations. In a coordinate system rotating with an angular velocity given by (3.3) for an eccentric roundabout all three vortices will remain fixed. In this section, we will determine the character of *perturbed* motion of vortices in the vicinity of stationary positions.

The Hamiltonian (2.10) in the system of coordinates rotating with the angular velocity (3.3) can be written as

$$\begin{aligned}\mathscr{H}(x_2^1, y_2^1, x_1^1, y_1^1, x_2^2, y_2^2) &= -\frac{1}{8\pi}\left\{\mu\left[F_1\left(\sqrt{(x_2^1-x_1^1)^2+(y_2^1-y_1^1)^2}\right)\right.\right.\\ &\left.+F_1\left(\sqrt{(x_2^2-x_1^1)^2+(y_2^2-y_1^1)^2}\right)\right]+F_2\left(\sqrt{(x_2^2-x_2^1)^2+(y_2^2-y_2^1)^2}\right)\\ &\left.-8\pi\frac{\omega}{4}\left[(x_2^1)^2+(y_2^1)^2+\mu\left((x_1^1)^2+(y_1^1)^2\right)+(x_2^2)^2+(y_2^2)^2\right]\right\},\end{aligned} \tag{4.1}$$

where

$$F_1(r)=\ln(r)+\mathrm{K}_0(r),\quad F_2(r)=\ln(r)-\mathrm{K}_0(r). \tag{4.2}$$

Note that the square-bracketed term multiplying ω in (4.1) is the total momentum, i.e. is constant. Consider small perturbations relative to the stationary configurations, satisfying (3.2). The coordinates of vortices are represented as

$$x_2^1=-B+\varepsilon_2^1,\quad y_2^1=\delta_2^1;\quad x_1^1=\varepsilon_1^1,\quad y_1^1=\delta_1^1;\quad x_2^2=2R-B+\varepsilon_2^2,\quad y_2^2=\delta_2^2, \tag{4.3}$$

where perturbations $\varepsilon_j^\alpha, \delta_j^\alpha \ll 1$ are chosen such that the total momentum (equal to zero in the coordinate system with origin at the vorticity centre) remains unchanged, i.e. the perturbed parts of the components of momentum satisfy the conditions

$$\Delta P_x=\tfrac{1}{2}(\varepsilon_2^1+\mu\varepsilon_1^1+\varepsilon_2^2)=0,\quad \Delta P_y=\tfrac{1}{2}(\delta_2^1+\mu\delta_1^1+\delta_2^2)=0. \tag{4.4}$$

In this case

$$\Delta M=\tfrac{1}{2}[(\varepsilon_2^1)^2+(\delta_2^1)^2+\mu((\varepsilon_1^1)^2+(\delta_1^1)^2)+(\varepsilon_2^2)^2+(\delta_2^2)^2]=C_1, \tag{4.5}$$

and

$$\Delta L=4Q\Delta M=\{\mu[(X_1)^2+(Y_1)^2+(X_3)^2+(Y_3)^2]+(X_2)^2+(Y_2)^2\}=C_2, \tag{4.6}$$

where C_1, C_2 are constants, and the following notation is introduced for projections of relative displacements of vortices:

$$\left.\begin{aligned}&X_1=\varepsilon_1^1-\varepsilon_2^1,\ Y_1=\delta_1^1-\delta_2^1,\quad X_2=\varepsilon_2^2-\varepsilon_2^1,\ Y_2=\delta_2^2-\delta_2^1,\\ &X_3=\varepsilon_2^2-\varepsilon_1^1,\ Y_3=\delta_2^2-\delta_1^1.\end{aligned}\right\} \tag{4.7}$$

Developing the expression for the Hamiltonian (4.1) to the second order in the coordinates of the relative perturbed motion, we obtain

$$\begin{aligned}\mathscr{H}(-B+\varepsilon_2^1,\delta_2^1;\varepsilon_1^1,\delta_1^1;2R-B+\varepsilon_2^2,\delta_2^2) &= -\frac{1}{8\pi}\cdots\\ -\frac{1}{16\pi}\left\{\left[\mu F_{1x_2^1x_2^1}(B)+F_{2x_2^1x_2^1}(2R)\right](\varepsilon_2^1)^2+\left[\mu F_{1x_2^2x_2^2}(2R-B)+F_{2x_2^2x_2^2}(2R)\right](\varepsilon_2^2)^2\right.\end{aligned}$$

$$+\mu\left[F_{1x_1^1x_1^1}(B)+F_{1x_1^1x_1^1}(2R-B)\right](\varepsilon_1^1)^2+2F_{2x_2^1x_2^2}(2R)\varepsilon_2^1\varepsilon_2^2+2\mu F_{1x_2^1x_1^1}(B)\varepsilon_2^1\varepsilon_1^1$$
$$+2\mu F_{1x_2^2x_1^1}(2R-B)\varepsilon_2^2\varepsilon_1^1+\left[\mu F_{1y_2^1y_2^1}(B)+F_{2y_2^1y_2^1}(2R)\right](\delta_2^1)^2+\left[\mu F_{1y_2^2y_2^2}(2R-B)\right.$$
$$\left.+F_{2y_2^2y_2^2}(2R)\right](\delta_2^2)^2+\mu\left[F_{1y_1^1y_1^1}(B)+F_{1y_1^1y_1^1}(2R-B)\right](\delta_1^1)^2+2F_{2y_2^1y_2^2}(2R)\delta_2^1\delta_2^2$$
$$\left.+2\mu F_{1y_2^1y_1^1}(B)\delta_2^1\delta_1^1+2\mu F_{1y_2^2y_1^1}(2R-B)\delta_2^2\delta_1^1\right\}. \tag{4.8}$$

The subscripts x_j^α and y_j^α denote derivatives with respect to this variables. We neglect both constant zero-order terms (including the term at ω), and all identically zero terms, in particular, first-order terms (because of the stationary character of the unperturbed configuration), and terms with mixed derivatives with respect to x_j^α and y_j^α that vanish at $y_j^\alpha=0$.

It can be readily shown that the derivatives satisfy the following relationships:

$$\begin{aligned}F_{nz_1^1z_1^1}(Z)&=F_{nz_2^2z_2^2}(Z)=F_{nz_2^1z_2^1}(Z)\\&=-F_{nz_1^1z_2^1}(Z)=-F_{nz_1^1z_2^2}(Z)=-F_{nz_2^1z_2^2}(Z)\\&=-\frac{1}{Z^2}+\mathrm{K}_0(Z)+\frac{\mathrm{K}_1(Z)}{Z}\equiv\Phi(Z),\end{aligned} \tag{4.9}$$

where $n=1,2$. Here z_j^α represents any variable of x_j^α or y_j^α and Z represents B, $2R$, or $2R-B$.

Now, considering (4.7) and (4.9), the quadratic part in the expansion of the Hamiltonian can be written as a function of the distance between perturbed positions of the vortices

$$\begin{aligned}&\mathscr{H}_2(X_1,Y_1;X_2,Y_2;X_3,Y_3)\\&\quad=\tfrac{1}{2}\left\{a\left[(X_1)^2+(Y_1)^2\right]+b\left[(X_2)^2+(Y_2)^2\right]+c\left[(X_3)^2+(Y_3)^2\right]\right\},\end{aligned} \tag{4.10}$$

where

$$[a,b,c]=-\frac{1}{8\pi}\left[\mu\Phi(B),\Phi(2R),\mu\Phi(2R-B)\right]. \tag{4.11}$$

To reduce this to a dynamic system with one degree of freedom, we apply Poisson brackets in the form

$$\begin{aligned}\{f,g\}=2\Bigg\{&\frac{\partial f}{\partial x_2^1}\frac{\partial g}{\partial y_2^1}-\frac{\partial f}{\partial y_2^1}\frac{\partial g}{\partial x_2^1}+\frac{1}{\mu}\left[\frac{\partial f}{\partial x_1^1}\frac{\partial g}{\partial y_1^1}-\frac{\partial f}{\partial y_1^1}\frac{\partial g}{\partial x_1^1}\right]\\&+\frac{\partial f}{\partial x_2^2}\frac{\partial g}{\partial y_2^2}-\frac{\partial f}{\partial y_2^2}\frac{\partial g}{\partial x_2^2}\Bigg\}\end{aligned} \tag{4.12}$$

to first integrals.

We will take into account the obvious consideration that a configuration of three vortices is always either a triangle or a segment, i.e. the projections of the distances between vortices are related by the expressions

$$X_1=\xi X_2,\quad X_3=(1-\xi)X_2,\quad Y_1=\zeta Y_2,\quad Y_3=(1-\zeta)Y_2. \tag{4.13}$$

Integrals (2.16) yield the equality

$$\mu BX_1+2RX_2+\mu(2R-B)X_3=0 \tag{4.14}$$

for all $\delta_j^\alpha = 0$. However, since, with the condition (3.2) taken into account, we have

$$\{\mathscr{H}_2, \mu B X_1 + 2RX_2 + \mu(2R - B)X_3\} = 0, \tag{4.15}$$

the equality (4.14) also holds for $\delta_j^\alpha \neq 0$, implying that

$$\xi = \frac{2R(1+\mu) - \mu B}{2\mu(R-B)}. \tag{4.16}$$

A similar expression for ζ can be derived from the trivial expression for the Poisson bracket for the quadratic part in the development of the Hamiltonian with an invariant $Y_1 - \zeta Y_2$:

$$\{\mathscr{H}_2, Y_1 - \zeta Y_2\} = [-\zeta\,(a\xi + 2b + c(1-\xi)) + (a\xi + \mu b - c(1-\xi))]\,X_2 = 0, \tag{4.17}$$

hence we have

$$\zeta = \frac{(1+\mu)a\xi + \mu b - c(1-\xi)}{\mu\,(a\xi + 2b + c(1-\xi))}. \tag{4.18}$$

From expressions (4.16) and (4.18), it follows that ξ and ζ can be considered constant in the context of development of the Hamiltonian to the second order. Now, using (4.6), we introduce two variables e_1 and e_2, which constitute a canonical pair and allow the action-angle variables to be determined in a natural way:

$$\frac{\Delta L}{\mu + 2} = (e_1)^2 + (e_2)^2, \tag{4.19}$$

where

$$(e_1)^2 = \frac{\mu\,(X_1)^2 + (X_2)^2 + \mu\,(X_3)^2}{\mu + 2}, \quad (e_2)^2 = \frac{\mu\,(Y_1)^2 + (Y_2)^2 + \mu\,(Y_3)^2}{\mu + 2}, \tag{4.20}$$

and the factor $1/(\mu+2)$ is introduced to make the (4.19) an equality of positive values, since $L \leqslant 0$ at $\mu \leqslant -2$. Now, using (4.13), we express the original variables and the quadratic part of the Hamiltonian in terms of variables (4.20):

$$\left(\frac{X_1}{\xi}\right)^2 = \left(\frac{X_3}{1-\xi}\right)^2 = (X_2)^2 = \frac{\mu+2}{\mu\xi^2 + 1 + \mu\,(1-\xi)^2}\,(e_1)^2, \tag{4.21a}$$

$$\left(\frac{Y_1}{\zeta}\right)^2 = \left(\frac{Y_3}{1-\zeta}\right)^2 = (Y_2)^2 = \frac{\mu+2}{\mu\zeta^2 + 1 + \mu\,(1-\zeta)^2}\,(e_2)^2, \tag{4.21b}$$

and

$$\mathscr{H}_2(e_1, e_2) = \frac{\mu+2}{2}\left[\frac{a\xi^2 + b + c\,(1-\xi)^2}{\mu\xi^2 + 1 + \mu\,(1-\xi)^2}\,(e_1)^2 + \frac{a\zeta^2 + b + c\,(1-\zeta)^2}{\mu\zeta^2 + 1 + \mu\,(1-\zeta)^2}\,(e_2)^2\right]. \tag{4.22}$$

The dynamic equations in the new variables become

$$\dot{e}_1 = \{\mathscr{H}_2, e_2\} = \tilde{\omega} e_2, \tag{4.23a}$$

$$\dot{e}_2 = \{\mathscr{H}_2, e_1\} = -\tilde{\omega} e_1, \tag{4.23b}$$

where

$$\tilde{\omega} = \frac{a\xi\zeta + b + c(1-\xi)(1-\zeta)}{\sqrt{\left(\mu\zeta^2 + 1 + \mu\,(1-\zeta)^2\right)\left(\mu\xi^2 + 1 + \mu\,(1-\xi)^2\right)}}. \tag{4.24}$$

Now, reducing the system of equations (4.23) to a second-order equation

$$\ddot{e}_1 = -\tilde{\omega}^2 e_1, \tag{4.25}$$

we see that $\tilde{\omega}$ is the frequency of the perturbed motion.

Thus, the solution of system (4.23) describes periodic oscillations with a frequency given by (4.24) along elliptic orbits with the principal semiaxis ratio of

$$\lambda = \frac{(e_1)_{max}}{(e_2)_{max}} = \sqrt{\frac{\mu\xi^2 + 1 + \mu\,(1-\xi)^2}{\mu\zeta^2 + 1 + \mu\,(1-\zeta)^2}}. \tag{4.26}$$

From (4.21) it follows that in differential relative coordinates, we have three ellipses with appropriate ratios:

$$\frac{(X_1)_{max}}{(Y_1)_{max}} = \frac{\xi}{\zeta}, \quad \frac{(X_2)_{max}}{(Y_2)_{max}} = 1, \quad \frac{(X_3)_{max}}{(Y_3)_{max}} = \frac{1-\xi}{1-\zeta}. \tag{4.27}$$

The shape of curves in the coordinates of relative motion x_j^α and y_j^α can be obtained by using (4.7) and (4.21):

$$\varepsilon_2^1 = -\frac{\mu X_1 + X_2}{\mu+2}, \quad \varepsilon_2^2 = \frac{-\mu X_1 + (1+\mu)X_2}{\mu+2}, \quad \varepsilon_1^1 = \frac{2X_1 - X_2}{\mu+2}, \tag{4.28a}$$

$$\delta_2^1 = -\frac{\mu Y_1 + Y_2}{\mu+2}, \quad \delta_2^2 = \frac{-\mu Y_1 + (1+\mu)Y_2}{\mu+2}, \quad \delta_1^1 = \frac{2Y_1 - Y_2}{\mu+2}. \tag{4.28b}$$

So, we obtain that, under the assumed approximation, the perturbed relative motions of vortices of the eccentric roundabout take place along elliptic orbits with semiaxis ratios

$$\frac{\left(\varepsilon_2^1\right)_{max}}{\left(\delta_2^1\right)_{max}} = \frac{\mu\xi + 1}{\mu\zeta + 1}, \quad \frac{\left(\varepsilon_2^2\right)_{max}}{\left(\delta_2^2\right)_{max}} = \frac{\mu(1-\xi) + 1}{\mu(1-\zeta) + 1}, \quad \frac{\left(\varepsilon_1^1\right)_{max}}{\left(\delta_1^1\right)_{max}} = \frac{2\xi - 1}{2\zeta - 1}, \tag{4.29}$$

and with the frequency given by (4.24).

Figure 6 gives the trajectories of relative motion in coordinates $\varepsilon_j^\alpha(t)$ and $\delta_j^\alpha(t)$ under the initial conditions

$$(x_2^1, y_2^1) = (-B_0 + \varepsilon_2^1, \delta_2^1), \quad (x_1^1, y_1^1) = (\varepsilon_1^1, \delta_1^1), \tag{4.30a}$$

$$(x_2^2, y_2^2) = (2R_0 - B_0 + \varepsilon_2^2, \delta_2^2), \tag{4.30b}$$

where B_0 and R_0 satisfy (3.2), and the lower branch of the curve in figure 5(*a*) is taken for all six cases. The values of ε_j^α, δ_j^α are given in the caption to figure 6.

It is obvious that by virtue of (4.28), the perturbation of the stationary position of at least one vortex induces appropriate deviations of the other two vortices, which is the idea of this figure. To facilitate the comparison of corresponding ellipses, their centres in the figure are aligned at $(0, 0)$. As shown in the figure, with the given external parameters, the trajectory of the vortex $\binom{1}{2}$ (here and below, the notation $\binom{\alpha}{i}$ is introduced for the point vortex with coordinates (x_i^α, y_i^α)) is nearly circular and has the maximal amplitude, while other vortices have the following properties: $(\varepsilon_1^1)_{max} > (\delta_1^1)_{max}$ and $(\varepsilon_2^2)_{max} < (\delta_2^2)_{max}$. With an increase in the absolute value of the top-layer-vortex intensity, the oscillation amplitudes of vortices $\binom{1}{1}$ and $\binom{2}{2}$ decrease. Note the interesting situation shown in figure 6(*ci*): here $(\delta_1^1)_{max} = (\delta_2^2)_{max}$.

In the case of a triton, from (4.17) and (4.18) we obtain

$$\xi = \zeta = \tfrac{1}{2}, \tag{4.31}$$

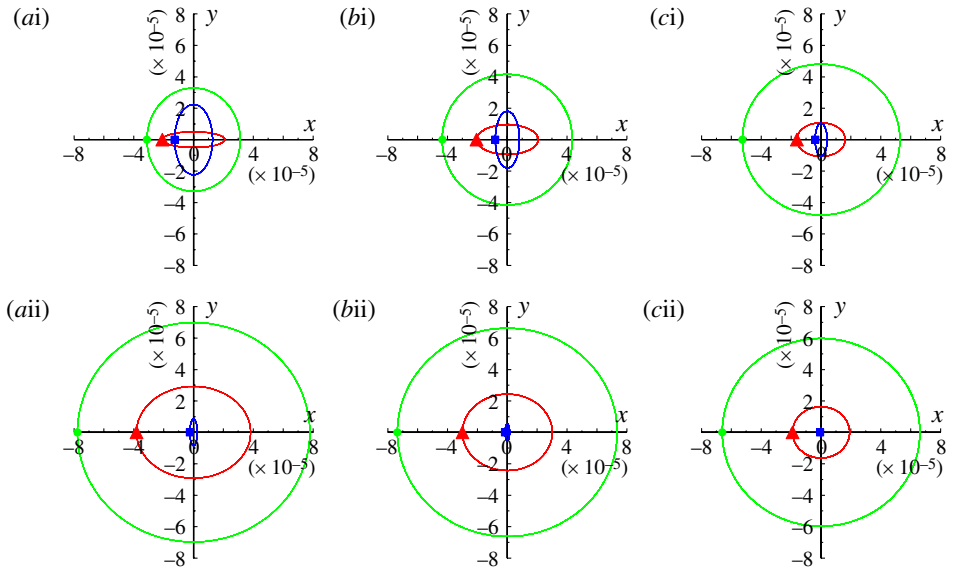

FIGURE 6. Trajectories of perturbed motions of point vortices in variables $\varepsilon_j^\alpha(t)$ and $\delta_j^\alpha(t)$ (the centres of ellipses were transferred to the system origin) with the initial conditions (4.30) at $\varepsilon_2^1 = -\varepsilon_2^2 = 2.5 \times 10^{-5}$, $\varepsilon_1^1 = \delta_1^1 = \delta_2^1 = \delta_2^2 = 0$. (i) $R_0 = 0.87$: (*a*i) $\mu = -2.1$, $B_0 = 0.2724$; (*b*i) $\mu = -2.5$, $B_0 = 0.1221$; (*c*i) $\mu = -3.5$, $B_0 = 0.0780$. (ii) $R_0 = 1.27$: (*a*ii) $\mu = -2.1$, $B_0 = 0.5021$; (*b*ii) $\mu = -2.5$, $B_0 = 0.0521$; (*c*ii) $\mu = -3.5$, $B_0 = 0.0271$. Symbols in the initial collinear configuration of vortices characterize the correspondence between trajectories and vortices as in figure 2.

i.e. all three ellipses are similar; therefore, we can take X_2, Y_2 as canonical variables and write the Hamiltonian as

$$\mathscr{H}_2(X_2, Y_2) = \frac{1}{2}\left(\frac{a}{4} + b + \frac{c}{4}\right)\left({X_2}^2 + {Y_2}^2\right), \tag{4.32}$$

where, in accordance with (4.11),

$$[a, b, c] = \frac{1}{4\pi}\left[\Phi(R), -\frac{1}{2}\Phi(2R), \Phi(2R - B)\right]. \tag{4.33}$$

Now, we readily obtain the frequency of the quasi-elliptic motions of the vortices constituting the perturbed triton:

$$\tilde{\omega}(R, B, -2) = \frac{a}{4} + b + \frac{c}{4}. \tag{4.34}$$

The same expression can be derived taking the limit of (4.24) for $\mu \to -2$, if we take into account that at the same time $\xi, \zeta \to 1/2$.

It is important to note that the frequencies (4.24) and (4.34), generally speaking, have non-zero limits $\tilde{\omega}_e$ at zero amplitudes ($\varepsilon_j^i = \delta_j^i = 0$). The dependence of the limiting frequencies (eigenfrequencies) of a perturbed motion on the size of the configuration R is illustrated in figure 7. The absolute values of frequencies increase with increasing R and $|\mu|$ for all $\mu < -1$, and the direction of rotation changes its sign at $\mu = -2$. Clearly, the conditions (3.2) or (3.6) hold on all curves.

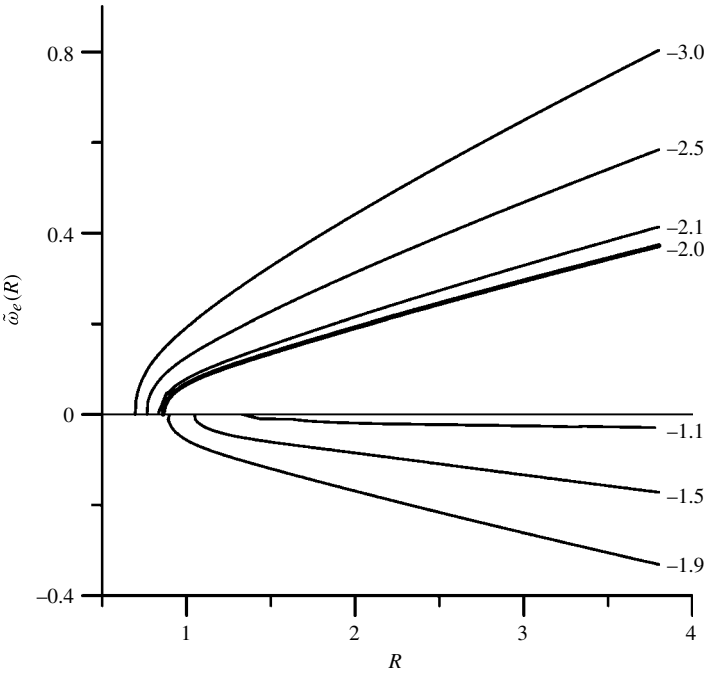

FIGURE 7. The eigenfrequencies of unperturbed motions $\tilde{\omega}_e$ at the specified values of parameter μ versus the initial size of configuration R. The thick line shows the case of $\mu = -2$ (triton).

The equality $\tilde{\omega}_e(R, B, \mu) = 0$ will be attained only in degenerate *static* states at $B = R_\mu$. In this case, for a roundabout, according to (3.4), we have $X_c = Y_c = 0$.

5. Analysis of perturbed motion at finite deviations from stationary states

It is clear that when deviations from stationary states are finite, the trajectories of vortices will have a form other than elliptic. Moreover, as was shown in § 2, the relative motions themselves may belong to different types {1}, {2}, or {3} (see figures 2 and 8).

Note their main properties.

(*a*) Type {1} – double capture, when all three vortices are involved in simultaneous rotational motion. Such motion can be conventionally denoted (Meleshko & Konstantinov 1993) by the scheme

$$\binom{1}{1}\binom{1}{2}\binom{2}{2}. \tag{5.1}$$

(*b*) Type {2} – simple capture, when one of the bottom-layer vortices joins with the top-layer vortex, and one of the following formulae is valid:

$$\binom{1}{1}\binom{1}{2}+\binom{2}{2} \quad \text{or} \quad \binom{1}{1}\binom{2}{2}+\binom{1}{2}. \tag{5.2}$$

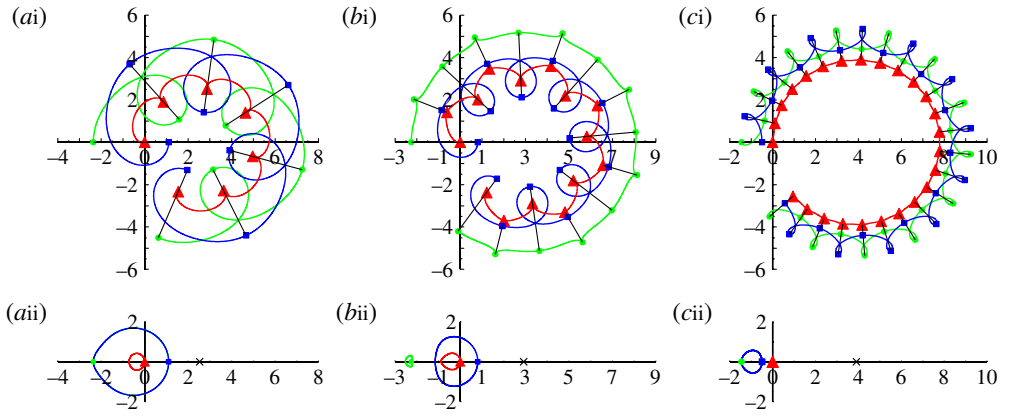

FIGURE 8. Examples of trajectories of absolute (i) and relative (ii) motions at $\mu = -2.5$: (*a*) type {1}, (*b*) type {2}, (*c*) type {3}. The red lines show the trajectories of the top-layer vortex $\binom{1}{1}$, and the green and blue lines show the trajectories of the bottom-layer vortices $\binom{1}{2}$ and $\binom{2}{2}$, respectively. The symbols are spaced by half period and the segments connecting them show synchronous (collinear) positions of the vortices. Crosses on the x-axis in (ii) show the coordinates of vorticity centres $(X_c, 0)$.

(*c*) Type {3} – the dominating factor is the within-layer interaction between the two bottom-layer vortices, and the motion of vortices is denoted by the scheme

$$\binom{1}{2}\binom{2}{2} + \binom{1}{1}. \tag{5.3}$$

It is significant that the relative motions of all three vortices are periodic and their trajectories are closed curves. Note that for relative motions of the type {1}, the trajectory of the upper-layer vortex is always located inside the 'choreography' (Simó 2001), performed by the bottom-layer vortices, and for motions of the type {3} it is outside it. This is illustrated by figure 8(*a*–*c*ii).

Numerical experiments for studying the absolute and relative motion of discrete vortices were carried out, solving (2.1)–(2.2) by the standard Bulirsch–Stoer method of fourth-order accuracy with initial conditions corresponding to the collinear arrangement of the three vortices.

A characteristic feature of relative motions of types {1} and {3} is that the bottom-layer vortices move periodically along a single trajectory, i.e. in the terms of Simó (2001), we have *complex choreographies*, and the ratio of rotation periods of the top-layer vortex to the bottom-layer vortices is 1/2. As mentioned in the previous section, the stationary states in the form of an eccentric roundabout belong to the class of motions {2}, which, in the general case, has the property that the top-layer vortex has a greater impact on one of the bottom-layer vortices than on the other. These stationary structures correspond to degenerate cases of equilibrium mutual influence of all three vortices.

The character of relative motions of vortices is demonstrated in more detail in figure 9, representing typical configurations of trajectories of all three types at a fixed value of parameter R (i.e. the distance between the bottom-layer vortices remaining constant from the initial moment) and variable B for $\mu = -2.5$. Clearly, the relative trajectories are obtained in a rotating coordinate system when the rotation centre is

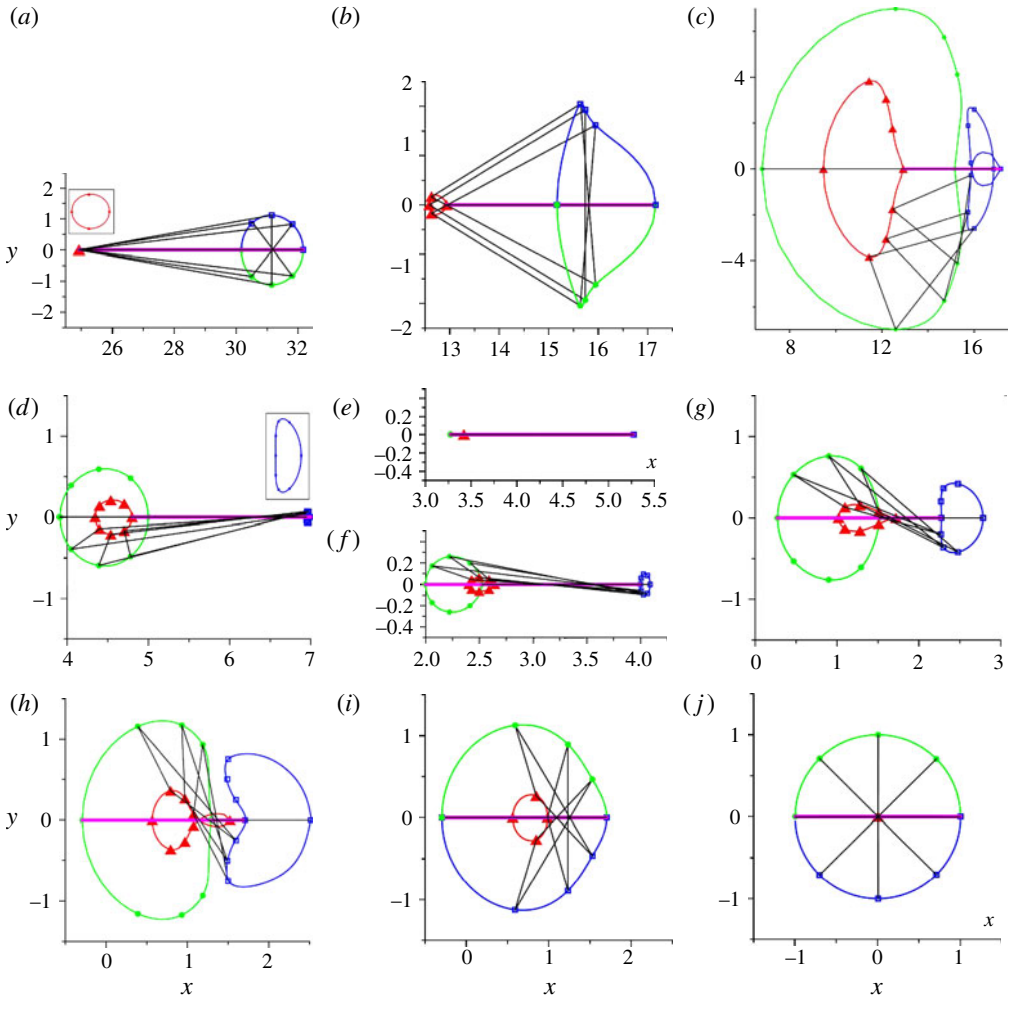

FIGURE 9. The relative trajectories (choreographies – for types {3} and {1}) of perturbed motions of point vortices with $R = 1$, $\mu = -2.5$ for the following values of B: (*a*) $B = -5.233$ (motion of type {3}), the amplitude of the top-layer vortex is exaggerated in the inset box; (*b*) $B = -2.233$ (motion of type {3}); (*c*) $B = -2.232$ (motion of type {2} – perturbed eccentric roundabout); (*d*) $B = -0.2$ (motion of type {2} – perturbed eccentric roundabout), the amplitude of one bottom-layer vortex is exaggerated in the inset box; (*e*) $B = 0.1452$ (motion of type {2} – eccentric roundabout); (*f*) $B = 0.4$ (motion of type {2} – perturbed eccentric roundabout); (*g*) $B = 0.745$ (motion of type {2} – perturbed eccentric roundabout); (*h*) $B = 0.858$ (motion of type {2} – perturbed eccentric roundabout); (*i*) $B = 0.859$ (motion of type {1} – perturbed ordinary roundabout); (*j*) $B = R = 1$ (motion of type {1} – ordinary roundabout). In each panel, the magenta segment corresponds to the initial state. The symbols have the same meaning as in figure 3.

located at the point (0, 0). Numerical experiments make it possible to follow the transformations of the vortex structure depending on the distance B between vortices $\binom{1}{1}$ and $\binom{1}{2}$.

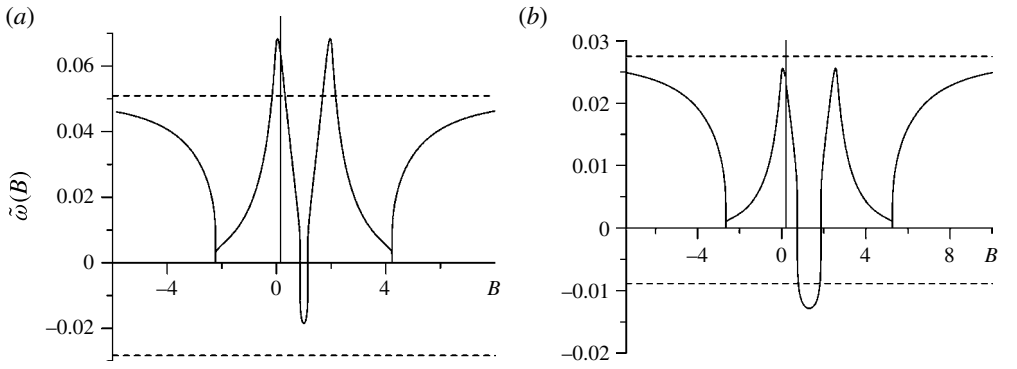

FIGURE 10. Turnover frequency of the perturbed motion $\tilde{\omega}$ versus B at: (a) $\mu = -2.5$, $R = 1$ and (b) $\mu = -1.5$, $R = 1.3$. The bottom dashed line denotes the turnover frequency of an ordinary roundabout $\tilde{\omega} = \omega_r$ at $B = R$ (3.1), and the top dashed line refers to the same case but at $\mu = 0$: $\tilde{\omega} = \omega_0$. The vertical lines correspond to the value $B = B_0$, and their intersection points with curves $\tilde{\omega}(B)$ are determined by the formula (4.24).

Unlike figure 8, where segments marked only collinear positions, in this case we show triangular configurations formed by vortices with a step of 1/8 period in an interval of 1/2 period. The insets where trajectories are given in a larger scale show the character of motion of individual vortices. The initial position everywhere corresponds to a collinear arrangement of vortices on the horizontal axis. In both cases, a progressive increase in parameter B, in accordance with figure 5, is accompanied by pathway $\{3\} \to \{2\} \to \{1\}$.

The analysis of these figures allows us to state that the asymptotic theory of § 4 has a wider application than that determined by formal criteria: the shape of vortex trajectories in figures 9(d) and 9(f) is not far from elliptic, notwithstanding the fact that the perturbations are not small. Obviously, even greater perturbations of the stationary structure (figures 9c and 9h) cause qualitative changes in the shape of trajectories up to self-intersection of curves. Nevertheless, all choreographies for motions of type {2} can be hereafter referred to as 'perturbed roundabouts'.

These illustrations are supplemented by figure 10, giving examples of frequency distributions for perturbed motions of the bottom-layer vortices as functions of parameter B given the values of R and μ. By the 'turnover' frequency, we mean the value $\tilde{\omega} = 2\pi/T$, where T is the period of vortex rotation along a closed trajectory. This variable is more convenient for analysis than the angular velocity, since it is constant for the given trajectory. It will be shown in KSV (see also Izrailsky, Koshel & Stepanov 2008; Koshel, Sokolovskiy & Davies 2008) that the analysis of the behaviour of fluid-particle turnover frequency along their trajectories is of use in studying chaotic advection in the vicinity of a vortex structure and in classification of possible types of movements.

Since the cases $B < R$ and $B > R$ are symmetrical, we will use the effect of the deviation of B from the dispersion value for the former case. With B great in magnitude, we have the motion of type {3}, where all three vortices move along nearly circular trajectories: oscillations in the top layer are very small (for this reason, in the inset, their amplitude is exaggerated), while in the bottom layer, the motion of vortices along the common trajectory is almost uniform and experiences almost no influence from the top-layer vortex (see figure 9a). As can be seen from figure 10, the frequency

of the perturbed motion is close to the turnover frequency of two identical vortices in the bottom layer and it is defined from (3.1) with $\mu = 0$.

The effect of the top-layer vortex on the dynamics in the bottom layer increases with decreasing absolute value of B. This results in a decrease in the frequency of the perturbed motion, a distortion of the shape of the curve along which bottom-layer vortices are moving, and an increase in the size of the domain it embraces.

Figure 9(*b*) gives trajectories close to limiting for this type of motion, while figure 10 gives the corresponding break points of curves $\tilde{\omega}(B)$, which are, at the same time, 'deceleration' points. In the phase portraits in figure 2, the initial conditions for this case correspond to the points of the phase domain boundary that belong to class {3} and lie near the separatrix, while the break point itself corresponds to the hyperbolic self-intersection point of the separatrix. This singular point corresponds to a configuration in the form of an immobile (in the rotating coordinate system) isosceles triangle; this configuration cannot form because of instability, though it 'tries' to form through the deceleration of vortices (see the beginning of § 3). In figure 10, the perturbed-motion frequency has local minima at these critical points.

The subsequent increase in the values of the governing parameter B by as little as 10^{-3} transfers the system into class {2} (figure 9*c*), where the top-layer vortex captures the nearest partner from the bottom layer, resulting in a qualitative change in the relative-motion topology. A characteristic feature of this type of motion is that each vortex has its individual trajectory. With an increase in parameter B, the amplitude characteristics of trajectories of all vortices change non-monotonically: first, they drop to zero values (the eccentric roundabout in figure 9*e*), and then they increase again.

However, an important distinction can be seen during a further increase in parameter B: the trajectory of the top-layer vortex, while still remaining a smooth curve, partially moves beyond the trajectory of its bottom-layer partner, after which a break appears in its configuration (this break can be clearly seen in figure 9*g*), serving as a nucleus for the formation of a doubly connected figure-eight structure.

During a further increase in B, the newly formed right-hand loop of the figure-eight, after reaching some limiting size, starts decreasing and disappears, thus making the curve simply connected again. In this process, the trajectories of bottom-layer vortices first are tangent and next merge, leading us to motions of type {1} (figure 9*i*), where the top-layer vortex permanently lies within the common trajectory of bottom-layer vortices. This takes place when the curve $\tilde{\omega}(B)$ crosses the axis $\tilde{\omega} = 0$ in figure 10(*a*).

When $B = R$, we have an ordinary symmetric roundabout with a static central vortex. Clearly, in figure 10(*a*), this situation corresponds to central extreme points.

Note that with B great in magnitude, the vorticity centre (3.4) is far from the three-vortex structure; with increasing R, the centre approaches this structure, penetrating into the segment connecting the bottom-layer vortices, and, finally, coincides with the top-layer vortex at $B = R$.

We have shown that with deviation from stationary configurations, the perturbed motion becomes periodic, and, in the case of an eccentric roundabout, there are two different frequencies – those of relative motion and rotation of the vortex structure as a whole.

It can be supposed that in this case there is no coordinate system in which the motion is steady. Thus, to describe the motion of fluid particles in a non-steady velocity field induced by a three-vortex system, we have a dynamical system with one and a half degrees of freedom. In this case, the motion of particles can become chaotic (Koshel & Prants 2006; Zaslavsky 2007; Koshel *et al.* 2008). An example of such behaviour will be given in KSV.

6. Summary and concluding remarks

Some issues of the dynamics of steady and quasi-steady three-vortex structures have been considered in the context of a two-layer, quasi-geostrophic model. A particular case of a three-vortex system was considered with two vortices having equal intensities and belonging to the bottom layer and the third vortex belonging to the top layer and having an arbitrary intensity of the opposite sign.

A large class of steady states with three vortices forming a collinear configuration referred to as an *eccentric roundabout* and rotating with a constant angular velocity about the vorticity centre was identified for such structures. Equation (3.1) is a necessary and sufficient condition for stationarity of such vortex structures; this is a particular dispersion relation linking the intensity of the upper-layer vortex with the distance between the vortices. A graphic solution of this equation may be constructed in a plane of parameters (B, R) for any $\mu : -2 > \mu > -\infty$ and $-1 \geqslant \mu > -2$. The example of the curve $B(R)$ when $\mu = -2.5$ is given in figure 5.

In the particular case of zero total intensity ($\mu = -2.0$), when the vorticity centre is at infinity, the motion of the collinear structure of three vortices is uniform and rectilinear. Such a construction is referred to as a *triton*. Note that the relative trajectories as well as the frequency dependences for the triton qualitatively have the same form as for the roundabout (figures 9 and 10).

It is shown that at small perturbations of the stationarity conditions, the vortices oscillate, moving along quasi-elliptic trajectories about their stationary positions. Section 4 demonstrates the relative vortex motions representing oscillations around the equilibrium positions along the quasi-elliptic trajectories in the vicinity of these stable stationary states. So, we can consider these base states to occupy a finite volume of the phase space.

The analysis of phase portraits, constructed in trilinear coordinates, has shown that only three qualitatively different types of motion for the case of finite perturbations are possible, depending on the degree of reciprocal influence of vortices belonging to the upper and lower layers. A classification of possible motions of such vortex structures and numerical calculations is given for the case of any finite perturbation.

Ryzhov & Koshel (2010) have shown that a regular area, whose outer boundary can be interpreted as the boundary of a finite-core vortex patch, is always formed around a point vortex. This result gives us reason to state that the results obtained here in the model of discrete vortices may be applied to finite-size vortices, and so may be used when interpreting characteristics of vortex interactions in the ocean and atmosphere.

Acknowledgements

This study was supported by RFBR (projects 13-05-00463, 13-05-00131, 11-05-00025), RFBR/CNRS (project 11-05-91052), RF Ministry of Education (Analytical Departmental Goal-Oriented Program ‘Development of the Scientific Potential of Higher School’, project 2.1.1/554). The authors are grateful to the four anonymous referees for their helpful comments on the manuscript.

REFERENCES

Aref, H. 1979 Motion of three vortices. *Phys. Fluids* **22**, 393–400.

Aref, H. 1983 Integrable, chaos and turbulent vortex motion in two-dimensional flows. *Annu. Rev. Fluid Mech.* **15**, 345–389.

Aref, H. 1986 The numerical experiment in fluid mechanics. *J. Fluid Mech.* **173**, 15–41.

AREF, H. 1989 Three-vortex motion with zero total circulation: addendum. *Z. Angew. Math. Phys.* **40**, 495–500.

AREF, H. 2009 Stability of relative equilibria of three vortices. *Phys. Fluids* **21**, 094101.

AREF, H. 2010 Self-similar motion of three point vortices. *Phys. Fluids* **22**, 057104.

AREF, H., JONES, S. W., MOFINA, S. & ZAWADSKI, I. 1989 Vortices, kinematics and chaos. *Physica* D **37**, 423–440.

AREF, H. & POMPHREY, N. 1980 Integrable and chaotic motions of four vortices. *Phys. Lett.* A **78**, 297–300.

AREF, H. & POMPHREY, N. 1982 Integrable and chaotic motions of four vortices. I. The case of identical vortices. *Proc. R. Soc. Lond.* A **380**, 359–387.

AREF, H. & STREMLER, M. A. 1999 Four-vortex motion with zero total circulation and impulse. *Phys. Fluids* **11**, 3704–3715.

BLACKMORE, D., TING, L. & KNIO, O. 2007 Studies of perturbed three vortex dynamics. *J. Math. Phys.* **48**, 065402.

BOGOMOLOV, V. A. 1977 Vorticity dynamics on a sphere. *Fluid Dyn.* **6**, 57–65.

BOGOMOLOV, V. A. 1985 On motion on a rotating sphere. *Izv. Acad. Nauk SSSR Atmos. Ocean. Phys.* **21**, 391–396.

BORISOV, A. V. & MAMAEV, I. S. 2005 *Mathematical Methods of Dynamics of Vortex Structures*. Institute of Computer Sciences.

BOYLAND, P., STREMLER, M. & AREF, H. 2003 Topological fluid mechanics of point vortex motions. *Physica* D **175**, 69–95.

ECKHARDT, B. 1988 Integrable four vortex motion. *Phys. Fluids* **31**, 2796–2801.

ECKHARDT, B. & AREF, H. 1988 Integrable and chaotic motions of four vortices. II. Collision dynamics of vortex pairs. *Phil. Trans. R. Soc. Lond.* A **326**, 655–696.

GRÖBLI, W. 1877 *Specialle Probleme ünber die Bewegung Geradliniger Paralleler Wirbelfäden*. Züricher und Furrer.

GRYANIK, V. M. 1983 Dynamics of singular geostrophic vortices in a two-layer model of the atmosphere (ocean). *Izv. Acad. Nauk SSSR Atmos. Ocean. Phys.* **19**, 227–240.

GRYANIK, V. M. 1988 Localized vortical disturbances – 'vortex charges' and 'vortex threads' in a baroclinic differentially rotating fluid. *Izv. Acad. Nauk SSSR Atmos. Ocean. Phys.* **24**, 1251–1261.

GRYANIK, V. M., SOKOLOVSKIY, M. A. & VERRON, J. 2006 Dynamics of heton-like vortices. *Regul. Chaot. Dyn.* **11**, 383–434.

GUDIMENKO, A. I. 2008 Dynamics of perturbed equilateral and collinear configurations of three point vortices. *Regul. Chaot. Dyn.* **13**, 85–95.

GUDIMENKO, A. I. & ZAKHARENKO, A. D. 2010 Qualitative analysis of relative motion of three vortices. *Russ. J. Non-linear Dyn.* **6**, 307–326 (in Russian).

HOGG, N. G. & STOMMEL, H. M. 1985 The heton, an elementary interaction between discrete baroclinic geostrophic vortices, and its implications concerning eddy heat-flow. *Proc. R. Soc. Lond.* A **397**, 1–20.

IZRAILSKY, YU. G., KOSHEL, K. V. & STEPANOV, D. V. 2008 Determination of optimal excitation frequency range in background flows. *Chaos* **18**, 013107.

JAMALOODEEN, M. I. & NEWTON, P. K. 2007 Two-layer quasigeostrophic potential vorticity model. *J. Math. Phys.* **48**, 065601.

KIMURA, Y. 1988 Chaos and collapse of a system of point vortices. *Fluid Dyn. Res.* **3**, 98–104.

KIZNER, Z. 2006 Stability and transitions of hetonic quartets and baroclinic modons. *Phys. Fluids* **18**, 056601.

KOSHEL, K. V. & PRANTS, S. V. 2006 Chaotic advection in the ocean. *Physics-Uspekhi (Advances in Physical Sciences)* **49**, 1151–1178.

KOSHEL, K. V., SOKOLOVSKIY, M. A. & DAVIES, P. A. 2008 Chaotic advection and nonlinear resonances in an oceanic flow above submerged obstacle. *Fluid Dyn. Res.* **40**, 695–736.

KOSHEL, K. V., SOKOLOVSKIY, M. A. & VERRON, J. 2013 Three-vortex quasi-geostrophic dynamics in a two layer fluid. Part 2. Regular and chaotic advection around the perturbed steady states. *J. Fluid Mech.* **717**, 255–280.

KOZLOV, V. V. 1998 *General Theory of Vortices*. Izd. dom Udmurtskii Universitet.

KOZLOV, V. V. 1996 *Symmetries, Topology and Resonances in Hamiltonian Mechanics*. Springer.

LAMB, H. 1932 *Hydrodynamics*, 6th edn. Dover.

MELESHKO, V. V. & VAN HEIJST, G. J. F. 1994 Interacting two-dimensional vortex structures: point vortices, contour kinematics and stirring properties. *Chaos, Solitons Fractals* **4**, 977–1010.

MELESHKO, V. V. & KONSTANTINOV, M. YU. 1993 *Dynamics of Vortex Structures*, p. 280. Naukova Dumka.

MELESHKO, V. V., KONSTANTINOV, M. YU., GURZHI, A. A. & KONOVALJUK, T. P. 1992 Advection of a vortex pair atmosphere in a velocity field of point vortices. *Phys. Fluids* A **4**, 2779–2797.

NEWTON, P. K. 2001 *The N-vortex Problem. Analytical Techniques. Applied Mathematical Sciences Series,* vol. 145, Springer.

NOVIKOV, E. A. 1976 Dynamics and statistics of a system of vortices. *Sov. Phys. JETP* **41**, 937–943.

NOVIKOV, E. A. & SEDOV, YU. B. 1979*a* Stochastic properties of a four-vortex system. *Sov. Phys. JETP* **48**, 440–444.

NOVIKOV, E. A. & SEDOV, YU. B. 1979*b* Stochastization of vortices. *J. Expl Theor. Phys. Lett.* **29**, 677–679.

POINCARÉ, H. 1893 *Theorie des Tourbillons*. G. Carré.

ROTT, N. 1989 Three-vortex motion with zero total circulation. *Z. Angew. Math. Phys.* **40**, 473–494.

ROTT, N. 1990 Constrained three- and four-vortex problems. *Phys. Fluids* A **2**, 1477–1480.

RYZHOV, E. A. & KOSHEL, K. V. 2010 Chaotic transport and mixing of a passive admixture by vortex flows behind obstacles. *Izv. Acad. Nauk SSSR Atmos. Ocean. Phys.* **46**, 184–191.

SIMÓ, K. 2001 New families of solutions to the N-body problem. In *Proc. ECM 2000, Barcelona. Progress in Mathematics*, vol. 201. pp. 101–115. Birkhäuser.

SOKOLOVSKIY, M. A., KOSHEL, K. V. & CARTON, X. 2010 Baroclinic multipole evolution in shear and strain. *Geophys. Astrophys. Fluid Dyn.* **105**, 506–535.

SOKOLOVSKIY, M. A. & VERRON, J. 2000*a* Finite-core hetons: stability and interactions. *J. Fluid Mech.* **423**, 127–154.

SOKOLOVSKIY, M. A. & VERRON, J. 2000*b* Four-vortex motion in the two layer approximation: integrable case. *Regul. Chaot. Dyn.* **5**, 413–436.

SOKOLOVSKIY, M. A. & VERRON, J. 2002*a* New stationary solutions of the three-vortex problem in a two-layer fluid. *Dokl. Phys.* **47**, 233–237.

SOKOLOVSKIY, M. A. & VERRON, J. 2002*b* Dynamics of the triangular two-layer vortex structures with zero total intensity. *Regul. Chaot. Dyn.* **7**, 435–472.

SOKOLOVSKIY, M. A. & VERRON, J. 2004 Dynamics of the three vortices in two-layer rotating fluid. *Regul. Chaot. Dyn.* **9**, 417–438.

SOKOLOVSKIY, M. A. & VERRON, J. 2006 Some properties of motion of $A + 1$ vortices in a two-layer rotating fluid. *Russ. J. Non-linear Dyn.* **2**, 27–54 (in Russian).

STREMLER, M. A. & AREF, H. 1999 Motion of three point vortices in a periodic parallelogram. *J. Fluid Mech.* **392**, 101–128.

SYNGE, J. L. 1949 On the motion of three vortices. *Can. J. Maths* **1**, 257–270.

TAVANTZIS, J. & TING, L. 1988 The dynamics of three vortices revisited. *Phys. Fluids* **31**, 1392–1409.

ZASLAVSKY, G. M. 2007 *The Physics of Chaos in Hamiltonian Systems*, 2nd edn. p. 316. Imperial College Press.

ZIGLIN, S. L. 1980 Nonintegrability of a problem on the motion of four point vortices. *Sov. Math. Dokl.* **21**, 296–299.